arXiv:1501.02455v2 [cond-mat.quant-gas] 19 Jan 2015

Magnetic Order Driven Topological Transition in the Haldane-Hubbard Model

Wei Zheng,[1] Huitao Shen,[1] Zhong Wang,[1,*] and Hui Zhai[1,†]

[1] *Institute for Advanced Study, Tsinghua University, Beijing, 100084, China*

(Dated: March 3, 2022)

In this letter we study the Haldane model with on-site repulsive interactions at half-filling. We show that the mean-field Hamiltonian with magnetic order effectively modifies parameters in the Haldane Hamiltonian, such as sublattice energy difference and phase in next nearest hopping. As interaction increases, increasing of magnetic order corresponds to varying these parameters and consequently, drives topological transitions. At the mean-field level, one scenario is that the magnetic order continuously increases, and inevitably, the fermion gap closes at the topological transition point with nonzero magnetic order. Beyond the mean-field, interaction between fermions mediated by spin-wave fluctuations can further open up the gap, rendering a first-order transition. Another scenario is a first-order transition at mean-field level across which a canted magnetic order develops discontinuously, avoiding the fermion gap closing. We find that both scenarios exist in the phase diagram of the Haldane-Hubbard model. Our predication is relevant to recent experimental realization of the Haldane model in cold atom system.

Correlation and topology are two of central topics in modern condensed matter physics. The Hubbard model of spin-1/2 fermions with on-site interaction is one of the most famous model that gives rise to highly nontrivial correlation effects, such as antiferromangetic order at half-filling. This model is relevant to many strongly correlated materials such as High-T_c cuprate superconductors. Recently, this model has also been simulated by using ultracold fermions in optical lattices [1–3]. In 1988, Haldane proposed a model of noninteracting fermions in the honeycomb lattice, which can give rise to topological band structure and quantized Hall conductance without external magnetic field [4]. This effect is now known as the quantum anomalous Hall effect, and has been observed experimentally in magnetically doped topological insulators [5]. The Haldane model has also been realized recently in cold atom experiment using shaking lattice technique [6, 7].

Motivated by recent cold atom realization of the Haldane model, in this letter we study the Haldane-Hubbard (HH) model of spin-1/2 fermions. In this model each spin component experiences the same single-particle Hamiltonian described by the Haldane model. At half-filling ($N_\uparrow = N_\downarrow = N_{\rm s}/2$, $N_{\rm s}$ is the number of sites), the system is a topological band insulator in the noninteracting limit. We consider only on-site repulsive interaction between two spin components as in the Hubbard model. In the strongly interacting limit, the system will enter a Mott insulator phase. Therefore, as interaction increases, we expect that two things will happen: One is the development of certain magnetic order, and the other is the transition from a topological band insulator to a topologically trivial Mott insulator. A natural question is how these two phenomena influence each other. The study of this question will shed light on the interplay between correlation and topology [8]. Previously, although there have been considerable interests focusing on the Kane-Mele-Hubbard model [9], the HH model is much less investigated [10].

In this letter we show that, at the mean-field level the magnetic order can drive a topological transition, either by a continuous second-order transition with fermion gap closed at finite magnetic order, or by a first-order transition with a jump of magnetic order parameter. Within the mean-field calculations, we show that both scenarios exist in the phase diagram of the HH model. We then go beyond the mean field by considering fluctuations of magnetic order. We show that for the former case, the spin-wave fluctuations generate effective interaction among gapless fermions at the nominal critical point of topological transition. This interaction, if sufficiently strong, can open up a gap and drives the transition to first-order.

The Model. We consider the HH model on a honeycomb lattice whose Hamiltonian is given by

$$\hat{H}_{\rm HH} = \hat{H}_{\rm H} + U\sum_i \hat{n}_{i,\uparrow}\hat{n}_{i,\downarrow} \tag{1}$$

$$\hat{H}_{\rm H} = -t_1\sum_{\langle ij\rangle,s}\left(\hat{c}^\dagger_{i,s}\hat{c}_{j,s} + {\rm h.c.}\right) - t_2\sum_{\langle\langle ij\rangle\rangle,s}\left(e^{i\phi_{ij}}\hat{c}^\dagger_{i,s}\hat{c}_{j,s} + {\rm h.c.}\right) - M\sum_{i,s}\epsilon_i\hat{c}^\dagger_{i,s}\hat{c}_{i,s} \tag{2}$$

where $s = \pm$ refers to spin up and down, respectively, the t_2-term represents next nearest hopping with a nontrivial phase $\phi_{ij} = \pm\phi$ for different sublattices, and the M-term adds a potential imbalance between A and B sub lattices, as $\epsilon_i = \pm 1$ for i belonging to A or B sublattices. The t_2 term breaks time-reversal symmetry, and the M-term breaks the inversion symmetry. Both terms open up the gap at Dirac points, and for half-filling, a phase diagram (without the interaction term) including a topological transition from trivial insulator to topologically nontrivial insulator is shown in Fig. 1(a), across which the gap at one of the Dirac point is closed. For the topologically nontrivial insulator, each spin compo-

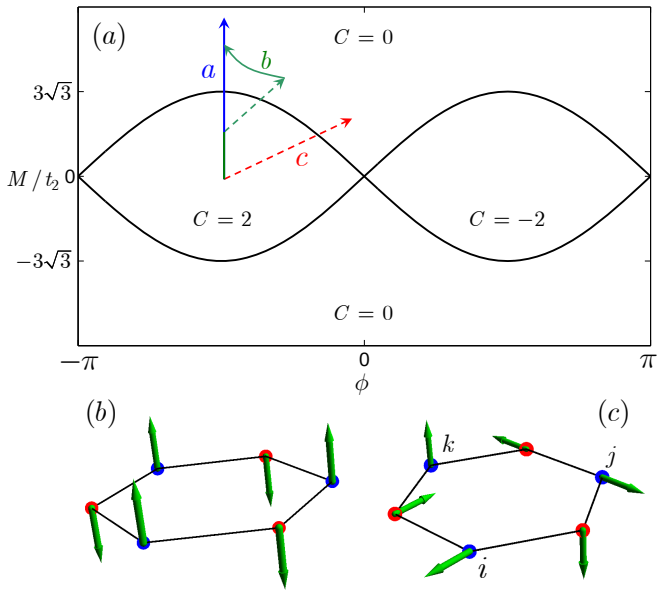


FIG. 1: (a) Phase diagram for the noninteracting Haldane Hamiltonian $\hat{H}_{\rm H}$ (Eq. 2), in terms of AB sublattice energy imbalance M and phase ϕ. The three trajectories labelled by a, b and c correspond to the evolution of mean-field Hamiltonian $\hat{H}_{\rm MF}$ (Eq. 4) with the increasing of magnetic order, as U/t_1 increases, for different t_2/t_1 as labelled by (a-c) in Fig. 2. The solid line means continuous evolution while the dashed line means discontinuous jump. Panels (b) and (c) illustrate two types of AF magnetic order: (b) is collinear AF order and (c) is canted AF order with nonzero spin chirality.

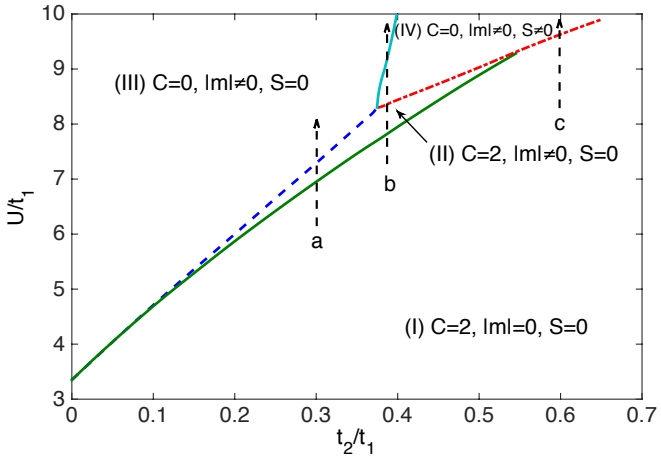


FIG. 2: Mean-field phase diagram for HH model in the $(t_2/t_1, U/t_1)$ plane. The green solid line is a second-order transition between a topological band insulator (Phase I) and a topological collinear AF insulator (Phase II). The blue dashed line is a topological transition between Phase II and a topological trivial collinear AF insulator (Phase III). The red dash-dot line is a first-order transition between either Phase I or Phase II and a topological trivial canted AF insulator (Phase IV). The blue solid line is a second-order phase transition between Phase III and Phase IV. Here (a-c) label three trajectories discussed in Fig. 1 and Fig. 3

nent fills the lower band with Chern number equalling 1 and the total Chern number $\mathcal{C} = 2$. The interaction term can be decoupled as

$$U\sum_i \hat{n}_{i,\uparrow}\hat{n}_{i,\downarrow} = \frac{1}{2}U\hat{N} - \frac{2}{3}U\sum_i \mathbf{S}_i^2$$
$$\approx \frac{1}{2}U\hat{N} + \sum_i \left(-\mathbf{m}_i\cdot\mathbf{S}_i + \frac{3\mathbf{m}_i^2}{8U}\right), \qquad (3)$$

where we have introduced an on-site magnetic order parameter $4U\langle\hat{\mathbf{S}}_i\rangle/3 = \mathbf{m}_i$. Thus the mean-field Hamiltonian $H_{\rm MF}$ is given by

$$\hat{H}_{\rm MF} = \hat{H}_{\rm H} - \sum_i \mathbf{m}_i\cdot\mathbf{S}_i. \qquad (4)$$

Relation between AF order and Topology. Before proceeding to the self-consistent mean-field calculation, we would like to first discuss the relation between the following two types of possible AF order and the parameters in the Haldane model.

(A) Collinear AF order, i.e. $\mathbf{m}_i = \mathbf{m}$ on the sublattice A and $\mathbf{m}_i = -\mathbf{m}$ on the sublattice B, as shown in Fig. 1(b). Due to the spin rotational symmetry, we can always choose $\mathbf{m} = m\hat{z}$. Thus, it adds a spin-dependent contribution on M in the single-particle Haldane model of Eq. 2, i.e. $M \to M + sm$, where $s = \pm$ denotes spin.

(B) Canted AF order. For simplicity, we consider the situation that $\mathbf{m}$ are different among the three A sites (denoted by i, j and k) of one honeycomb, as shown in Fig. 1(c), which leads to finite "scalar spin chirality" order $\mathcal{S} = \langle\hat{\mathbf{S}}_i\rangle\cdot(\langle\hat{\mathbf{S}}_j\rangle\times\langle\hat{\mathbf{S}}_k\rangle)$ (Since we are concerned with magnetically ordered state, we do not use the usual definition, i.e. $\langle\mathbf{S}_i\cdot(\mathbf{S}_j\times\mathbf{S}_k)\rangle$.). Within each unit cell, $\mathbf{m}_i$ at A site is approximately opposite to $\mathbf{m}_i$ at B site.

Then we can apply an on-site spin rotation U_i so that $U_i^\dagger(\mathbf{m}_i\cdot\mathbf{S}_i)U_i = \frac{1}{2}|\mathbf{m}_i|s_{iz}$ for A sublattices and $U_i^\dagger(\mathbf{m}_i\cdot\mathbf{S}_i)U_i = -\frac{1}{2}|\mathbf{m}_i|s_{iz}$, where s_{iz} is the Pauli matrix associated to spin. Qualitatively speaking, this local spin rotation introduces an additional Berry phase factor $\pm\tilde{\phi}$ in the next nearest hopping term for different sublattices, where $\tilde{\phi}$ is approximately one sixth of the solid angle expanded by $\mathbf{m}_i, \mathbf{m}_j, \mathbf{m}_k$, that is to say, ϕ in the original Haldane Hamiltonian Eq. 2 should be replaced by an effective phase $\phi_{\rm eff} = \phi + \tilde{\phi}$.

Therefore, the mean-field Hamiltonian with a collinear AF order corresponds to a free-fermion Hamiltonian $\hat{H}_{\rm H}$ with a modified spin-dependent effective M, and the mean-field Hamiltonian with a canted AF order corresponds to a free-fermion Hamiltonian with both M and ϕ in $\hat{H}_{\rm H}$ modified. Thus, the noninteracting phase diagram in Fig. 1(a) is helpful for understanding the mean-field phases, with M and ϕ replaced by effective parameters determined by magnetic order. There emerge two different scenarios about how magnetic orders drive transition

between topological nontrivial and trivial insulators.

(i) If AF order increases continuously as interaction strength U increases, the mean-field Hamiltonian will evolve continuously cross the phase boundary from $\mathcal{C}=2$ to $\mathcal{C}=0$ insulator. Inevitably, there will be a topological transition at which gapless fermions and a finite AF order coexist.

(ii) A first-order transition occurs as U increases, at which a jump of AF order brings the system from $\mathcal{C}=2$ regime in the phase diagram to $\mathcal{C}=0$ regime.

Mean-field Phase Diagram. A self-consistent mean-field calculation is conducted to determine the phase diagram. For simplicity, we first consider the situation with $M=0$ and $\phi=\pi/2$ in $\hat{H}_{\rm H}$ in Eq. 2. In our calculation, we enlarge the unit cell to six sites of each honeycomb, and no further assumption for order parameter $\mathbf{m}_i$ at these six sites are imposed. (i.e. totally 18 parameters are determined from self-consistent iterations.) Enlarging the unit cell in the magnetic ordered phase turns out to be crucial for obtaining the state with lower energy and establishing the correct picture as discussed below. After we obtain the self-consistent solution, we can straightforwardly compute the single-particle gap for fermions, scalar spin chirality order and the Chern number for mean-field ground state [12]. The resulting phase diagram is shown in Fig. 2, which contains both two scenarios of phase transition, depending on the ratio t_2/t_1, as well as four different phases: I. topological band insulator with no AF order ($|\mathbf{m}|=0$, $\mathcal{C}=2$); II. topological AF insulator with collinear AF order ($|\mathbf{m}|\neq 0$, $\mathcal{C}=2$ and $\mathcal{S}=0$); III. trivial AF insulator with collinear AF order ($|\mathbf{m}|\neq 0$, $\mathcal{C}=0$ and $\mathcal{S}=0$), and IV. trivial AF insulator with canted AF order ($|\mathbf{m}|\neq 0$, $\mathcal{C}=0$ and $\mathcal{S}\neq 0$).

First, for small t_2/t_1, such as the trajectory labelled by (a) in Fig. 2, as U/t_1 increases, the system first undergoes a second-order phase transition across which a collinear AF order develops continuously (Fig. 3(a1)). As such a magnetic order increases, the mean-field Hamiltonian $H_{\rm MF}$ acquires a M ($-M$) term for spin-up (down), which suppresses the single particle gap at K (K') point (Fig. 3(a2)). Thus, $H_{\rm MF}$ undergoes a trajectory as labeled by (a) in Fig. 1(a). As $|\mathbf{m}|$ increases to a certain value, the single particle gap closes at K (K') point, beyond which the mean-field ground becomes a topological trivial one (i.e. $\mathcal{C}=0$, Fig. 3(a3)). Along this trajectory, the spin chirality $\mathcal{S}$ is always zero (Fig. 3(a4)).

Secondly, for intermediate t_2/t_1, such as the trajectory labelled by (b) in Fig. 2, as U/t_1 increases, the system first develops a collinear AF order (Fig. 3(b1)). Then, instead of reaching a topological transition, the system undergoes a first-order transition across which the magnetic order becomes canted. This is accompanied by a jump of spin chirality order $\mathcal{S}$ (Fig. 3 (b4)). This corresponds to a discontinuous change of effective M and ϕ in $\hat{H}_{\rm MF}$, as shown by trajectory labeled by (b) in Fig. 1(a). Consequently, the system jumps from a topological phase

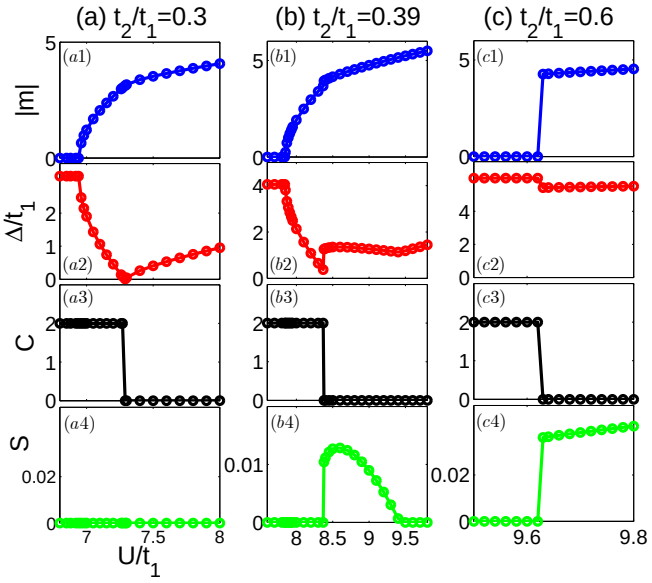


FIG. 3: The magnetic order $|\mathbf{m}|$, gap of fermion excitation Δ, Chern number $\mathcal{C}$ and scalar spin chirality order $\mathcal{S}$ as a function of U/t_1 for three different value of t_2/t_1, as labeled by (a-c) in Fig. 2.

to a topological trivial phase (Fig. 3(b3)), and the gap closing point is avoided (Fig. 3(b2)). This canted AF order can also be understood by a ring-exchange spin model in term of local spin picture. As U/t_1 further increases, the effective ring exchange is suppressed, $\mathcal{S}$ gradually decreases and the system returns to a collinear AF insulator (Fig. 3(b4)).

Finally, for large t_2/t_1, such as the trajectory labelled by (c) in Fig. 2, as U/t_1 increases, a first-order transition directly brings the system from a topological band insulator to a trivial canted AF insulator, across which $|\mathbf{m}|$, $\mathcal{C}$, $\mathcal{S}$ all display discontinuity (Fig. 3(c1),(c3),(c4)), and the fermion gap Δ remains finite all through (Fig. 3(c2)).

Fluctuations Beyond Mean-field. Here we focus on the topological transition from Phase II to Phase III, at which the gapless fermions coexist with gapless Goldstone spin-wave mode of AF order. This invites the question whether the spin-wave fluctuation will change the critical behavior. To answer this question, we introduce the following low-energy theory with action

$$S=\int dtd^2\mathbf{r}\left(\mathcal{L}_{\rm n}+\mathcal{L}_{\rm f}+\mathcal{L}_{\rm I}\right) \tag{5}$$

$$\mathcal{L}_{\rm n}=\frac{1}{2g}\left[(\partial_t\mathbf{n})^2-c^2(\nabla\mathbf{n})^2\right] \tag{6}$$

$$\mathcal{L}_{\rm f}=\Psi^\dagger\left[i\partial_t+iv_{\rm F}\tau_z\sigma_x\partial_x+iv_{\rm F}\sigma_y\partial_y-m\tau_z\sigma_z\right]\Psi \tag{7}$$

$$\mathcal{L}_{\rm I}=-\lambda\Psi^\dagger[\sigma_z\otimes(\mathbf{n}\cdot\mathbf{s})]\Psi. \tag{8}$$

where $\mathcal{L}_{\rm n}$ is a nonlinear sigma model that describes the low-energy fluctuation of AF Néel order $\mathbf{n}$, and the eight-component object $\Psi\equiv\Psi_{\alpha s\sigma}$ describes the Dirac fermion

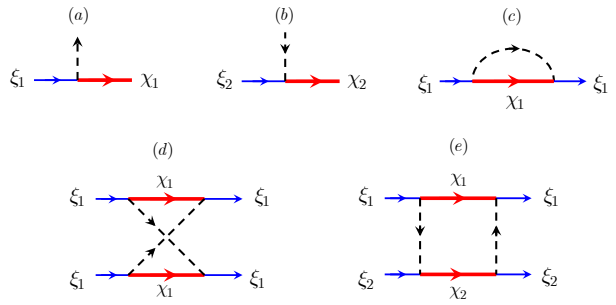


FIG. 4: The spin-wave-fermion vertices are shown in (a,b), and the self-energy correction for the low energy fermions is shown in (c). The induced interaction among gapless fermions is shown in (d,e). The thin solid lines are the gapless fermion ξ_κ and the thick solid lines are the gapped fermions χ_κ. The dashed line represents spin-wave $\varphi \equiv n_x + in_y$.

nearby two valleys at K and K' points, in which $s =\uparrow (\downarrow)$ denotes the spin up (down), $\alpha = 1, 2$ denotes the valley, and $\sigma = A(B)$ denotes the sublattice. The Pauli matrices $s_{x,y,z}$, $\sigma_{x,y,z}$, and $\tau_{x,y,z}$ refer to the spin, sublattice, and valley degrees of freedom, respectively. The parameters c and $v_{\rm F}$ are the spin-wave and fermion velocities, respectively. Parameters g and λ are coupling constants of spin fluctuation and coupling between spin and fermions, respectively. Here c, $v_{\rm F}$, g, m and λ can all be given by microscopic parameters. In particular, in Eq.7 the mass m is given by $m = 3\sqrt{3}t_2$.

With collinear AF order, we can assume that $\langle \mathbf{n} \rangle$ is ordered along $\hat{z}$ direction, and then take $n_z = 1$ and expand the action to the linear order of n_x and n_y, $\varphi = n_x + in_y$ representing a complex gapless boson field. To bring $\mathcal{L}$ into a more convenient form, we implement a local spin rotation $\Psi(\mathbf{x}, t) \to U(\mathbf{x}, t)\Psi(\mathbf{x}, t)$, with $U = \exp[i(n_y s_x - n_x s_y)/2 + \cdots]$, such that $U^\dagger(\mathbf{n} \cdot \mathbf{s})U = s_z$. Since this rotation involves only fermions, the $\mathcal{L}_{\rm n}$ term is unchanged, while $\mathcal{L}_{\rm f} + \mathcal{L}_{\rm I}$ becomes

$$\mathcal{L}_{\rm f} + \mathcal{L}_{\rm I} = \Psi^\dagger \left[iD_t + iv_{\rm F}\tau_z\sigma_x D_x + iv_{\rm F}\sigma_y D_y - m\sigma_z\tau_z - \lambda\sigma_z s_z \right] \Psi, \qquad (9)$$

where the covariant derivative $iD_\mu = i\partial_\mu - \frac{i}{2}(s_+\partial_\mu\varphi^* - s_-\partial_\mu\varphi)$, in which $s_\pm = \frac{1}{2}(s_x \pm is_y)$ and $\mu = t, x, y$. Thus, the mass term becomes $-\Psi^\dagger\sigma_z \otimes (m\tau_z \otimes I + \lambda I \otimes s_z)\Psi$, where I denotes 2×2 identity matrix. It is therefore clear that when $\lambda = m$, namely, at the mean-field critical point, $\Psi_{1\downarrow}$ and $\Psi_{2\uparrow}$ become gapless (the sublattice index σ is suppressed). Hereafter we shall define $\xi_1 \equiv \Psi_{1\downarrow}$ and $\xi_2 \equiv \Psi_{2\uparrow}$, which are gapless fermions, and $\chi_1 \equiv \Psi_{1\uparrow}$ and $\chi_2 \equiv \Psi_{2\downarrow}$, which are gapped fermions.

The low-energy spin waves have small momentum, therefore the spin-wave-fermion interaction given by D_μ terms does not change the valley index, i.e. by interacting with spin waves, ξ_κ can only turn into χ_κ with same κ (Fig. 4(a,b)). After integrating out the spin-wave and the gapped fermions χ_κ, we can obtain a self-energy correction for low-energy fermions ξ_κ, as well as effective interactions among the massless fermions [12], with corresponding diagrams shown in Fig. 4(d-e). To the lowest order the self-energy takes the form of $\Sigma\tau_z\sigma_z$. Thus, it merely shifts the phase boundary. The induced interaction reads

$$\hat{V} = \int \frac{d^3k_1}{(2\pi)^3}\frac{d^3k_2}{(2\pi)^3}\frac{d^3q}{(2\pi)^3}V_q \Big[\sum_{\kappa=1,2} (\xi^\dagger_{\kappa,k_1-q}\sigma_z\xi_{\kappa,k_1}) \times(\xi^\dagger_{\kappa,k_2+q}\sigma_z\xi_{\kappa,k_2}) - 2(\xi^\dagger_{1,k_1-q}\sigma_z\xi_{1,k_1})(\xi^\dagger_{2,k_2+q}\sigma_z\xi_{2,k_2}) \Big] \qquad (10)$$

where $q = (\omega, \mathbf{q})$, d^3q is a shorthand notation for $\int d\mathbf{q}d\omega$, and similarly for d^3k. Neglecting the q dependence of $V(q)$, we have $V(q) = -u \equiv -(1/2)^4 g^2 c\Lambda^3/6\pi^2 m^2$ under certain approximation[12], where Λ is a momentum cutoff.

This spin-wave-induced interaction, if sufficiently strong, can open up a gap at the nominal critical point. To see this fact, we only need to do a mean-field approximation of $\hat{V}$. We find that if $u > u_c \equiv \pi v_F/\Lambda$, the gapless "ground-state" at $\lambda = m$ is unstable towards the dynamical generation[11] of a mass term $\pm\Delta\xi^\dagger\sigma_z s_z\xi$, with $\Delta = \pi v_F^2(1/u_c - 1/u)$. Away from the $\lambda = m$ point, the $-$ sign (+ sign) in $\pm\Delta\xi^\dagger\sigma_z s_z\xi$ is selected at $\lambda = m + 0^+$ ($\lambda = m - 0^+$). That is to say, the generated mass jumps by 2Δ across the mean-field transition point $\lambda = m$, thus, the nominal gap closing of fermions is avoided, and the transition becomes a first-order one.

Finally, we remark that this physics triggered by massless spin-wave has no counterpart in the Kane-Mele-Hubbard model, because the $SU(2)$ spin rotational symmetry is explicitly broken there, thus the Goldstone mode is absent therein.

Final remarks. Recent cold atom realization of the Haldane model can be naturally described by this HH model. In fact, in the experiment reported in Ref. [6], Mott insulator with suppressed double-occupancy sites has been observed. Our theoretical predications can be directly verified in this setup. In this realization, since the most crucial next nearest hopping term is generated by periodically shaking optical lattices, the periodic driving will also modify the interaction term, in the order of $1/\omega$ (ω is shaking frequency). The thermal fluctuation of magnetic order may also be important. These effects will be left for future investigations.

We would like to thank Yi-Zhuang You, Hong Yao, Fa Wang and Shou-Cheng Zhang for discussions. This work is supported by Tsinghua University Initiative Scientific Research Program, NSFC under Grant No. 11304175 (ZW), No. 11325418 (HZ), No. 11174176 (HZ), and NKBRSFC under Grant No. 2011CB921500 (HZ).

Note added: Upon finishing this work, we became aware of Ref.[13], in which the same model is studied.

* Electronic address: wangzhongemail@gmail.com
† Electronic address: hzhai@mail.tsinghua.edu.cn

[1] R. Jördens, N. Strohmaier, K. Günter, H, Moritz and T. Esslinger, Nature **455**, 204 (2008).
[2] U. Schneider, L. Hackermller, S. Will, Th. Best, I. Bloch, T. A. Costi, R. W. Helmes, D. Rasch, Science **322**, 1520 (2008)
[3] R. A. Hart, P. M. Duarte, T.-L. Yang, X. Liu, T. Paiva, E. Khatami, R. T. Scalettar, N. Trivedi, D. A. Huse, R. G. Hulet, arXiv: 1407.5932
[4] F. D. M. Haldane, Phys. Rev. Lett. 61, 2015 (1988)
[5] C.-Z. Chang, J. Zhang, X. Feng, J. Shen, Z. Zhang, M. Guo, K. Li, Y. Ou, P. Wei, L.-L. Wang, Z.-Q. Ji, Y. Feng, S. Ji, X. Chen, J. Jia, X. Dai, Z. Fang, S.-C. Zhang, K. He, Y. Wang, L. Lu, X.-C. Ma, and Q.-K. Xue, Science, **340** 167 (2013)
[6] G. Jotzu, M. Messer, R. Desbuquois, M. Lebrat, T. Uehlinger, D. Greif, and T. Esslinger, Nature, **515** 237 (2014)
[7] This scheme was proposed by: T. Oka and H. Aoki, Phys. Rev. B 79, 081406 (2009), and W. Zheng and H. Zhai, Phys. Rev. A 89, 061603 (2014).
[8] S. Raghu, X.-L. Qi, C. Honerkamp, and S.-C. Zhang, Phys. Rev. Lett. 100, 156401 (2008); A. Shitade, H. Katsura, J. Kune, X.-L. Qi, S.-C. Zhang, and N. Nagaosa, Phys. Rev. Lett. 102, 256403 (2009); Y. Zhang, Y. Ran, and A. Vishwanath, Phys. Rev. B 79, 245331 (2009); Z. Wang, X.-L. Qi, and S.-C. Zhang, Phys. Rev. Lett. 105, 256803 (2010); D. A. Pesin and Leon Balents, Nature Phys. 6, 376 (2010); L. Fidkowski and A. Kitaev, Phys. Rev. B 81, 134509 (2010); M. Dzero, K. Sun, V. Galitski, and P. Coleman, Phys. Rev. Lett. 104, 106408 (2010); Z. Wang and S.-C. Zhang, Phys. Rev. X 2, 031008 (2012); S. Rachel and K. Le Hur, Phys. Rev. B 82, 075106 (2010); F. Lu, J. Zhao, H. Weng, Z. Fang, and X. Dai, Phys. Rev. Lett. 110, 096401 (2013); A. Ruegg and G. A. Fiete, Phys. Rev. Lett. 108, 046401 (2012); A. Go, W. Witczak-Krempa, G. S. Jeon, K. Park, and Y. B. Kim, Phys. Rev. Lett. 109, 066401 (2012); A. Amaricci, J. C. Budich, M. Capone, B. Trauzettel, and G. Sangiovanni, arXiv:1411.7390v1.
[9] D. Zheng, G.-M. Zhang, and C. Wu, Phys. Rev. B 84, 205121 (2011); M. Hohenadler, T. C. Lang, and F. F. Assaad, Phys. Rev. Lett. 106, 100403 (2011); S.-L. Yu, X. C. Xie, and J.-X. Li, Phys. Rev. Lett. 107, 010401 (2011). H.-H. Hung, L. Wang, Z.-C. Gu, and G. A. Fiete, Phys. Rev. B 87, 121113(R) (2013); T. C. Lang, A. M. Essin, V. Gurarie, and S. Wessel, Phys. Rev. B 87, 205101 (2013); J. C. Budich, R. Thomale, G. Li, M. Laubach, and S.-C. Zhang, Phys. Rev. B 86, 201407(R) (2012); M. Hohenadler, Z. Y. Meng, T. C. Lang, S. Wessel, A. Muramatsu, and F. F. Assaad, Phys. Rev. B 85, 115132 (2012); C. Griset and C. Xu, Phys. Rev. B 85, 045123 (2012); Z. Y. Meng, H. H. Hung, T. C. Lang, Modern Phys. Lett. B Vol. 28, No. 1, 1430001 (2014); F. F. Assaad, M. Bercx, and M. Hohenadler, Phys. Rev. X 3, 011015 (2013); M. Hohenadler and F. F. Assaad, J. Phys.: Condens. Matter 25, 143201 (2013); J. C. Budich, B. Trauzettel, and G. Sangiovanni, Phys. Rev. B 87, 235104 (2013); M. Laubach, J. Reuther, R. Thomale, and S. Rachel, Phys. Rev. B 90, 165136 (2014); H.-H. Lai, H.-H. Hung, G. A. Fiete, Phys. Rev. B 90, 195120 (2014).
[10] J. He, S.-P. Kou, Y. Liang, and S. Feng, Phys. Rev. B 83, 205116 (2011); J. He, Y.-H. Zong, S.-P. Kou, Y. Liang, and S. Feng, Phys. Rev. B 84, 035127 (2011); Joseph Maciejko and Andreas Ruegg, Phys. Rev. B 88, 241101(R) (2013). These papers focus on different aspect of this model.
[11] Y. Nambu and G. Jona-Lasinio, Phys. Rev. 122, 345 (1961).
[12] See supplementary material for details of (i) self-consistent mean-field solution; and (ii) calculating Chern number $\mathcal{C}$ and scalar spin chirality $\mathcal{S}$ from the obtained ground state, and (iii) integrating out gapped fermion and spin-wave to obtain the low-energy theory for gapless fermions.
[13] C. Hickey, P. Rath, and A. Paramekanti, arXiv:1501.01304

SUPPLEMENTAL MATERIAL

Mean-field theory

The Hamiltonian of the Haldane-Hubbard model is given by

$$\begin{aligned}\hat{H} &= -t_1\sum_{\langle ij\rangle,s}\left(\hat{c}^\dagger_{i,s}\hat{c}_{j,s}+\text{h.c.}\right)-t_2\sum_{\langle\langle ij\rangle\rangle,s}\left(e^{i\phi_{ij}}\hat{c}^\dagger_{i,s}\hat{c}_{j,s}+\text{h.c.}\right)\\ &\quad -M\sum_{i,s}\epsilon_i\hat{c}^\dagger_{i,s}\hat{c}_{i,s}+U\sum_i\hat{n}_{i,\uparrow}\hat{n}_{i,\downarrow}.\end{aligned}\tag{11}$$

In the following we will only consider the $M=0$ case. At the mean-field level, we decompose the on-site interaction term as

$$U\sum_i\hat{n}_{i,\uparrow}\hat{n}_{i,\downarrow} = \frac{1}{2}U\hat{N}-\frac{2}{3}\sum_i\mathbf{S}_i^2 \tag{12}$$

$$\approx \frac{1}{2}U\hat{N}+\sum_i\left(-\mathbf{m}_i\cdot\mathbf{S}_i+\frac{3\mathbf{m}_i^2}{8U}\right), \tag{13}$$

where $\mathbf{S}_i = \frac{1}{2}\sum_{ss'}\hat{c}^\dagger_{i,s}\sigma_{ss'}\hat{c}_{i,s'}$ is the spin operator and $\mathbf{m}_i = 4U\langle\mathbf{S}_i\rangle/3$ is the on-site magnetic order parameter. The mean-field Hamiltonian can be constructed as

$$\begin{aligned}\hat{H}_{\mathrm{MF}} &= -t_1\sum_{\langle ij\rangle,s}\left(\hat{c}^\dagger_{i,s}\hat{c}_{j,s}+\mathrm{h.c.}\right)-t_2\sum_{\langle\langle ij\rangle\rangle,s}\left(e^{i\phi_{ij}}\hat{c}^\dagger_{i,s}\hat{c}_{j,s}+\mathrm{h.c.}\right)\\ &\quad-\sum_i\left\{m_i^z\left(\hat{c}^\dagger_{i,\uparrow}\hat{c}_{i,\uparrow}-\hat{c}^\dagger_{i,\downarrow}\hat{c}_{i,\downarrow}\right)+m_i^x\left(\hat{c}^\dagger_{i,\uparrow}\hat{c}_{i,\downarrow}+\hat{c}^\dagger_{i,\downarrow}\hat{c}_{i,\uparrow}\right)-im_i^y\left(\hat{c}^\dagger_{i,\uparrow}\hat{c}_{i,\downarrow}-\hat{c}^\dagger_{i,\downarrow}\hat{c}_{i,\uparrow}\right)\right\}. \end{aligned} \tag{14}$$

This Hamiltonian is quadratic form and can be directly diagonalized. As explained in the main text, we enlarge the unit cell to a full hexagon containing six sites. We do a Fourier transformation

$$\hat{c}_{\alpha,s}(\mathbf{k}) = \frac{1}{\sqrt{\mathcal{N}}}\sum_{\mathbf{R}} e^{-i\mathbf{k}\cdot\mathbf{R}}\hat{c}_{\alpha,\sigma}(\mathbf{R}),$$

where $\mathbf{R}$ is the position of the unit cell, $\alpha = A1, B1, A2, B2, A3, B3$ denote the sublattices and $\mathcal{N}$ is the total number of unit cells. The Hamiltonian can be transformed into momentum space:

$$\hat{H}_{\mathrm{MF}} = \sum_{\mathbf{k}\in\mathrm{BZ}}\Psi^\dagger(\mathbf{k})H(\mathbf{k})\Psi(\mathbf{k}), \tag{15}$$

where $\Psi^\dagger(\mathbf{k})$ is a 12-component spinor:

$$\Psi^\dagger(\mathbf{k}) = \left(\hat{c}^\dagger_{A1,\uparrow},\hat{c}^\dagger_{B1,\uparrow},\hat{c}^\dagger_{A2,\uparrow},\hat{c}^\dagger_{B2,\uparrow},\hat{c}^\dagger_{A3,\uparrow},\hat{c}^\dagger_{B3,\uparrow},\hat{c}^\dagger_{A1,\downarrow},\hat{c}^\dagger_{B1,\downarrow},\hat{c}^\dagger_{A2,\downarrow},\hat{c}^\dagger_{B2,\downarrow},\hat{c}^\dagger_{A3,\downarrow},\hat{c}^\dagger_{B3,\downarrow}\right) \tag{16}$$

Diagonalizing the matrix $H(\mathbf{k})$, one can obtain the energy band for the mean-field Hamiltonian

$$\sum_{ij}U^\dagger_{\mu i}H_{ij}(\mathbf{k})U_{j\nu} = \delta_{\mu\nu}E_\mu(\mathbf{k}). \tag{17}$$

Therefore the diagonalized mean-field Hamiltonian is

$$\hat{H}_{\mathrm{MF}} = \sum_{\mathbf{k}\in\mathrm{BZ}}\sum_\mu \Phi^\dagger_\mu(\mathbf{k})E_\mu(\mathbf{k})\Phi_\mu(\mathbf{k}),$$

where $\Phi_\mu(\mathbf{k}) = \sum_i U^\dagger_{\mu i}\Psi_i(\mathbf{k})$ is the fermion operator of each band. For the half-filling case, the ground state is the full-filling of the lowest 6 bands,

$$|\mathrm{GS}\rangle = \prod_{\mu=1}^{6}\prod_{\mathbf{k}\in\mathrm{BZ}}\Phi^\dagger_\mu(\mathbf{k})|0\rangle. \tag{18}$$

The magnetization $\mathbf{m}_\alpha$ can be calculated from the ground state as

$$\begin{aligned} m^z_\alpha &= \frac{1}{2\mathcal{N}}\sum_{\mathbf{k}\in\mathrm{BZ}}\left\langle\hat{c}^\dagger_{\alpha,\uparrow}(\mathbf{k})\hat{c}_{\alpha,\uparrow}(\mathbf{k})-\hat{c}^\dagger_{\alpha,\downarrow}(\mathbf{k})\hat{c}_{\alpha,\downarrow}(\mathbf{k})\right\rangle_{\mathrm{GS}},\\ m^x_\alpha &= \frac{1}{2\mathcal{N}}\sum_{\mathbf{k}\in\mathrm{BZ}}\left\langle\hat{c}^\dagger_{\alpha,\uparrow}(\mathbf{k})\hat{c}_{\tau,\downarrow}(\mathbf{k})-\hat{c}^\dagger_{\alpha,\downarrow}(\mathbf{k})\hat{c}_{\alpha,\uparrow}(\mathbf{k})\right\rangle_{\mathrm{GS}},\\ m^y_\alpha &= \frac{1}{2i\mathcal{N}}\sum_{\mathbf{k}\in\mathrm{BZ}}\left\langle\hat{c}^\dagger_{\alpha,\uparrow}(\mathbf{k})\hat{c}_{\tau,\downarrow}(\mathbf{k})+\hat{c}^\dagger_{\alpha,\downarrow}(\mathbf{k})\hat{c}_{\alpha,\uparrow}(\mathbf{k})\right\rangle_{\mathrm{GS}}. \end{aligned}$$

Since there are six sites in each unit cell, one has to self-consistently calculate 18 parameters of $\mathbf{m}_\alpha$. We numerically calculate the ground state and iterate until the magnetization at each site converges. We then calculate the spin chirality order defined by

$$\mathcal{S} = \left\langle\hat{\mathbf{S}}_i\right\rangle\cdot\left(\left\langle\hat{\mathbf{S}}_j\right\rangle\times\left\langle\hat{\mathbf{S}}_k\right\rangle\right),$$

The Chern number of interacting quantum anomalous Hall insulators has been defined in Ref.[1]. At the mean-field level it is reduced to the Chern number of the mean-field wavefunction. We numerically calculate this Chern number using the algorithm given in Ref. [2].

Effective Field Theory

Near the phase boundary between Phase II to Phase III, we introduce the following low-energy thoery with action

$$\begin{aligned} S &= \int dtd^2\mathbf{r}\left(\mathcal{L}_{\rm n}+\mathcal{L}_{\rm f}+\mathcal{L}_{\rm I}\right), \\ \mathcal{L}_{\rm n} &= \frac{1}{2g}\left[\left(\partial_t\mathbf{n}\right)^2-c^2\left(\nabla\mathbf{n}\right)^2\right], \\ \mathcal{L}_{\rm f} &= \Psi^\dagger\left[i\partial_t+v_F\tau_z\sigma_x i\partial_x+v_F\sigma_y i\partial_y-m\tau_z\sigma_z\right]\Psi, \\ \mathcal{L}_{\rm I} &= -\lambda\Psi^\dagger\left[\sigma_z\otimes\left(\mathbf{n}\cdot\mathbf{s}\right)\right]\Psi. \end{aligned}$$

The parameters are explained in the text. With the collinear AF order, we can assume that the $\mathbf{n}$ is ordered along $\hat{z}$, direction, namely, $\vec{n}\approx(0,0,1)$. We expand $\mathcal{L}_n$ to the linear order of n_x and n_y as

$$\mathcal{L}_{\rm n}=\frac{1}{2g}\sum_{i=x,y}\left[\left(\partial_t n_i\right)^2-c^2\left(\nabla n_i\right)^2\right]. \tag{19}$$

Then we make a spin rotation, $\Psi(x)\to U(x)\Psi(x)$, with $U(x)=\exp\left[i\left(n_y(x)s_x-n_x(x)s_y\right)/2+\cdots\right]$, such that

$$U^\dagger(x)\left(\mathbf{n}\cdot\mathbf{s}\right)U(x)=s_z.$$

Then the last term of the Lagrangian becomes

$$\mathcal{L}_{\rm I}=-\lambda\Psi^\dagger\left(\sigma_z\otimes s_z\right)\Psi. \tag{20}$$

It is a mass term of the fermions, so it could be absorbed into the action of fermions. We have $\mathcal{L}_{\rm f}+\mathcal{L}_{\rm I}$

$$\mathcal{L}_{\rm f}=\Psi^\dagger\left[iD_t+v_F\tau_z\sigma_x iD_x+v_F\sigma_y iD_y-m\tau_z\sigma_z-\lambda\sigma_z s_z\right]\Psi, \tag{21}$$

where the covariant derivative is given by:

$$\begin{aligned} D_\mu &= \partial_\mu+U^\dagger\partial_\mu U \\ &= \partial_\mu+\frac{1}{2}\left(s_-\partial_\mu\varphi-s_+\partial_\mu\varphi^*\right), \end{aligned}$$

where $s_\pm=\frac{1}{2}\left(s_x\pm is_y\right)$, and $\varphi=n_x+in_y$. This $\mathcal{L}_{\rm f}+\mathcal{L}_{\rm I}$ can be written explicitly as

$$\begin{aligned} \mathcal{L}_{\rm f} &= \Psi^\dagger_{1\uparrow}\left[i\partial_t+v_F\sigma_x i\partial_x+v_F\sigma_y i\partial_y-(m+\lambda)\sigma_z\right]\Psi_{1\uparrow}+\Psi^\dagger_{1\downarrow}\left[i\partial_t+v_F\sigma_x i\partial_x+v_F\sigma_y i\partial_y-(m-\lambda)\sigma_z\right]\Psi_{1\downarrow} \\ &+\Psi^\dagger_{2\uparrow}\left[i\partial_t-v_F\sigma_x i\partial_x+v_F\sigma_y i\partial_y+(m-\lambda)\sigma_z\right]\Psi_{2\uparrow}+\Psi^\dagger_{2\downarrow}\left[i\partial_t-v_F\sigma_x i\partial_x+v_F\sigma_y i\partial_y+(m+\lambda)\sigma_z\right]\Psi_{2\downarrow} \\ &+\frac{1}{2}\Psi^\dagger_{1\downarrow}\left(i\partial_t\varphi+v_F\sigma_x i\partial_x\varphi+v_F\sigma_y i\partial_y\varphi\right)\Psi_{1\uparrow}-\frac{1}{2}\Psi^\dagger_{1\uparrow}\left(i\partial_t\varphi^*+v_F\sigma_x i\partial_x\varphi^*+v_F\sigma_y i\partial_y\varphi^*\right)\Psi_{1\downarrow} \\ &+\frac{1}{2}\Psi^\dagger_{2\downarrow}\left(i\partial_t\varphi-v_F\sigma_x i\partial_x\varphi+v_F\sigma_y i\partial_y\varphi\right)\Psi_{2\uparrow}-\frac{1}{2}\Psi^\dagger_{2\uparrow}\left(i\partial_t\varphi^*-v_F\sigma_x i\partial_x\varphi^*+v_F\sigma_y i\partial_y\varphi^*\right)\Psi_{2\downarrow}. \end{aligned} \tag{22}$$

When $\lambda=m$, namely, at the mean field critical point, $\mathcal{L}_{\rm f}$ becomes

$$\begin{aligned} \mathcal{L}_{\rm f} &= \Psi^\dagger_{1\uparrow}\left[i\partial_t+v_F\sigma_x i\partial_x+v_F\sigma_y i\partial_y-2m\sigma_z\right]\Psi_{1\uparrow}+\Psi^\dagger_{1\downarrow}\left[i\partial_t+v_F\sigma_x i\partial_x+v_F\sigma_y i\partial_y\right]\Psi_{1\downarrow} \\ &+\Psi^\dagger_{2\uparrow}\left[i\partial_t-v_F\sigma_x i\partial_x+v_F\sigma_y i\partial_y\right]\Psi_{2\uparrow}+\Psi^\dagger_{2\downarrow}\left[i\partial_t-v_F\sigma_x i\partial_x+v_F\sigma_y i\partial_y+2m\sigma_z\right]\Psi_{2\downarrow} \\ &+\frac{1}{2}\Psi^\dagger_{1\downarrow}s_-\left(i\partial_t\varphi+v_F\sigma_x i\partial_x\varphi+v_F\sigma_y i\partial_y\varphi\right)\Psi_{1\uparrow}-\frac{1}{2}\Psi^\dagger_{1\uparrow}s_+\left(i\partial_t\varphi^*+v_F\sigma_x i\partial_x\varphi^*+v_F\sigma_y i\partial_y\varphi^*\right)\Psi_{1\downarrow} \\ &+\frac{1}{2}\Psi^\dagger_{2\downarrow}s_-\left(i\partial_t\varphi-v_F\sigma_x i\partial_x\varphi+v_F\sigma_y i\partial_y\varphi\right)\Psi_{2\uparrow}-\frac{1}{2}\Psi^\dagger_{2\uparrow}s_+\left(i\partial_t\varphi^*-v_F\sigma_x i\partial_x\varphi^*+v_F\sigma_y i\partial_y\varphi^*\right)\Psi_{2\downarrow}. \end{aligned} \tag{23}$$

We can see that $\Psi_{1\downarrow}$ and $\Psi_{2\uparrow}$ become gapless, while $\Psi_{1\uparrow}$ and $\Psi_{2\downarrow}$ are gapped. We redefine

$$\begin{aligned} \xi_1 &= \Psi_{1\downarrow},\ \xi_2=\Psi_{2\uparrow},\ \chi_1=\Psi_{1\uparrow},\ \chi_2=\Psi_{2\downarrow} \\ \bar{\xi}_1 &= \Psi^\dagger_{1\downarrow}\sigma_z,\ \bar{\xi}_2=\Psi^\dagger_{2\uparrow}\sigma_z,\ \bar{\chi}_1=\Psi^\dagger_{1\uparrow}\sigma_z,\ \bar{\chi}_2=\Psi^\dagger_{2\downarrow}\sigma_z \\ \varphi &= n_x+in_y,\ \varphi^*=n_x-in_y, \end{aligned}$$

then the total action becomes

$$\begin{aligned}
\mathcal{L}_{\mathrm{n}} &= \frac{1}{2g}\left(|\partial_t\varphi|^2 - c^2\left|\nabla\varphi\right|^2\right) \\
\mathcal{L}_{\mathrm{f}} &= \bar{\xi}_1\left(\gamma_0 i\partial_t + v_F\gamma_1 i\partial_x + v_F\gamma_2 i\partial_y\right)\xi_1 + \bar{\xi}_2\left(\gamma_0 i\partial_t - v_F\gamma_1 i\partial_x + v_F\gamma_2 i\partial_y\right)\xi_2 \\
&\quad + \bar{\chi}_1\left(\gamma_0 i\partial_t + v_F\gamma_1 i\partial_x + v_F\gamma_2 i\partial_y - 2m\right)\chi_1 + \bar{\chi}_2\left(\gamma_0 i\partial_t - v_F\gamma_1 i\partial_x + v_F\gamma_2 i\partial_y + 2m\right)\chi_2, \\
\mathcal{L}_{\mathrm{I}} &= \frac{1}{2}\bar{\xi}_1\left(\gamma_0 i\partial_t\varphi + v_F\gamma_1 i\partial_x\varphi + v_F\gamma_2 i\partial_y\varphi\right)\chi_1 - \frac{1}{2}\bar{\chi}_1\left(\gamma_0 i\partial_t\varphi^* + v_F\gamma_1 i\partial_x\varphi^* + v_F\gamma_2 i\partial_y\varphi^*\right)\xi_1 \\
&\quad + \frac{1}{2}\bar{\chi}_2\left(\gamma_0 i\partial_t\varphi - v_F\gamma_1 i\partial_x\varphi + v_F\gamma_2 i\partial_y\varphi\right)\xi_2 - \frac{1}{2}\bar{\xi}_2\left(\gamma_0 i\partial_t\varphi^* - v_F\gamma_1 i\partial_x\varphi^* + v_F\gamma_2 i\partial_y\varphi^*\right)\chi_2.
\end{aligned}$$

Note that we have mapped the low energy theory into four Dirac fields interacting with a complex scalar field. In the following, we will integrate out the massive Dirac fields and the complex scaler field to obtain an effective theory for the massless fermions.

The partition function is given by

$$Z = \int D\xi D\chi D\varphi e^{iS_\xi + iS_\chi + iS_\varphi + iS_{\mathrm{I}}}. \tag{24}$$

Integrating out the χ and φ field gives rise to an effective action for ξ field

$$e^{iS\mathrm{eff}} = e^{iS_\xi}\int D\chi D\varphi e^{iS_\chi + iS_\varphi + iS_{\mathrm{I}}} = e^{iS_\xi}\left\langle e^{iS_{\mathrm{I}}}\right\rangle_0, \tag{25}$$

Here $\left\langle e^{iS_{\mathrm{I}}}\right\rangle_0$ is the average over free χ and φ field, which reads

$$\begin{aligned}
\left\langle e^{iS_{\mathrm{I}}}\right\rangle_0 &= 1 - \frac{1}{2!}\left\langle S_{\mathrm{I}}^2\right\rangle + \frac{1}{4!}\left\langle S_{\mathrm{I}}^4\right\rangle + \cdots \\
&= \exp\left(-\frac{1}{2!}\left\langle S_{\mathrm{I}}^2\right\rangle + \frac{1}{4!}\left(\left\langle S_{\mathrm{I}}^4\right\rangle - 3\left\langle S_{\mathrm{I}}^2\right\rangle^2\right) + \cdots\right)
\end{aligned} \tag{26}$$

The effective action has the form of

$$S_{\mathrm{eff}} = S_\xi + \frac{i}{2!}\left\langle S_{\mathrm{I}}^2\right\rangle - \frac{i}{4!}\left(\left\langle S_{\mathrm{I}}^4\right\rangle - 3\left\langle S_{\mathrm{I}}^2\right\rangle^2\right). \tag{27}$$

The second term in Eq. 27 generates a self-energy for the gapless fermion, which is illustrated in fig.4 (c).

$$\frac{i}{2!}\left\langle S_{\mathrm{I}}^2\right\rangle = \int\frac{d^3p}{\left(2\pi\right)^3}\bar{\xi}_\kappa\left(p\right)\Sigma_\kappa\left(p\right)\xi_\kappa\left(p\right).$$

This self-energy has the form of

$$\begin{aligned}
\Sigma_{1,2}\left(p\right) &= i\int\frac{d^3k}{\left(2\pi\right)^3}\frac{\gamma_0 k_0 - v_F\gamma_1 k_1 - v_F\gamma_2 k_2}{2}iD\left(k\right)\frac{\gamma_0 k_0 - v_F\gamma_1 k_1 - v_F\gamma_2 k_2}{2}iK_{1,2}(p-k), &(28)\\
&= \frac{i}{4}\int\frac{d^3k}{\left(2\pi\right)^3}\left(k_0^2 - v_F^2k_1^2 - v_F^2k_2^2\right)D\left(k\right)K_{1,2}(p-k), &(29)
\end{aligned}$$

where $D\left(k\right)$ is the propagator of the complex scaler field, and $K_{1,2}(k)$ is the propagator of the massive Dirac fermions:

$$\begin{aligned}
D\left(k\right) &= \frac{2g}{k_0^2 - c^2k_1^2 - c^2k_2^2 + i\varepsilon} &(30)\\
K_{1,2}\left(k\right) &= \frac{1}{\gamma_0 k_0 \mp v_F\gamma_1 k_1 - v_F\gamma_2 k_2 \mp 2m + i\varepsilon}. &(31)
\end{aligned}$$

For low energy processes, we approximate $K_{1,2}\left(k\right) \approx \mp\frac{1}{2m}$, so that the self energy is given by:

$$\Sigma_{1,2}\left(p\right) = \mp\frac{ig}{4m}\int\frac{d^3k}{\left(2\pi\right)^3}\frac{k_0^2 - v_F^2k_1^2 - v_F^2k_2^2}{k_0^2 - c^2k_1^2 - c^2k_2^2 + i\varepsilon}, \tag{32}$$

One can see that it merely shifts the mean-field phase boundary without qualitatively changing its physical properties.

The third term in the effective action 27, as illustrated in fig.4 (d) and (e), generates an effective interaction between the gapless fermions:

$$-\frac{i}{4!}\left(\left\langle S_{\mathrm{I}}^{4}\right\rangle -3\left\langle S_{\mathrm{I}}^{2}\right\rangle ^{2}\right)=-\frac{1}{2}\int\frac{d^{3}q}{\left(2\pi\right)^{3}}\frac{d^{3}k_{1}}{\left(2\pi\right)^{3}}\frac{d^{3}k_{2}}{\left(2\pi\right)^{3}}V_{q}\left(\sum_{\kappa=1,2}\bar{\xi}_{\kappa,k_{1}-q}\bar{\xi}_{\kappa,k_{2}+q}\xi_{\kappa,k_{2}}\xi_{\kappa,k_{1}}-2\bar{\xi}_{1,k_{1}-q}\bar{\xi}_{2,k_{2}+q}\xi_{2,k_{2}}\xi_{1,k_{1}}\right),$$

where the V_q is given by:

$$\begin{aligned}V_{q} &= \frac{i}{2^{4}}\frac{1}{4m^{2}}\int\frac{d^{3}k}{\left(2\pi\right)^{3}}\\ &\quad\times\left(k_{0}^{2}-v_{F}^{2}k_{1}^{2}-v_{F}^{2}k_{2}^{2}\right)D\left(k\right)\left[\left(q_{0}+k_{0}\right)^{2}-v_{F}^{2}\left(q_{1}+k_{1}\right)-v_{F}^{2}\left(q_{2}+k_{2}\right)\right]D\left(q+k\right).\end{aligned}$$

When $q=0$, we have:

$$\begin{aligned}V_{0} &= \frac{i}{2^{4}}\frac{1}{4m^{2}}\int\frac{d^{3}k}{\left(2\pi\right)^{3}}\left(k_{0}^{2}-v_{F}^{2}k_{1}^{2}-v_{F}^{2}k_{2}^{2}\right)^{2}D^{2}\left(k\right).\\ &= \frac{ig^{2}}{2^{4}m^{2}}\int\frac{d^{3}k}{\left(2\pi\right)^{3}}\left(\frac{k_{0}^{2}-v_{F}^{2}k_{1}^{2}-v_{F}^{2}k_{2}^{2}}{k_{0}^{2}-c^{2}k_{1}^{2}-c^{2}k_{2}^{2}+i\varepsilon}\right)^{2}.\\ &= -\frac{g^{2}c\Lambda^{3}}{2^{4}\pi^{2}m^{2}}\left[\frac{1}{6}-\left(1-\frac{v_{F}^{2}}{c^{2}}\right)\frac{2}{9}+\left(1-\frac{v_{F}^{2}}{c^{2}}\right)^{2}\frac{4}{45}\right]\end{aligned}$$

where Λ is a momentum cutoff. This is the effective interaction between the fermions.

* Electronic address: wangzhongemail@gmail.com
† Electronic address: hzhai@mail.tsinghua.edu.cn

[1] Z. Wang and S.-C. Zhang, Phys. Rev. X 2, 031008 (2012)
[2] Takahiro Fukui, Yasuhiro Hatsugai, and Hiroshi Suzuki, J. Phys. Soc. Jpn. **74** (2005) pp. 1674-1677